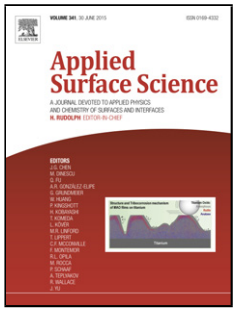

Title: Intermatrix Synthesis as a rapid, inexpensive and reproducible methodology for the *in situ* functionalization of nanostructured surfaces with Quantum Dots

Author: Julio Bastos-Arrieta Jose Muñoz Anja Stenbock-Fermor Maria Muñoz Dmitri N. Muraviev Francisco Céspedes Larisa A. Tsarkova Mireia Baeza

PII: S0169-4332(16)30138-6
DOI: http://dx.doi.org/doi:10.1016/j.apsusc.2016.01.277
Reference: APSUSC 32509

To appear in: *APSUSC*

Received date: 17-12-2015
Revised date: 27-1-2016
Accepted date: 31-1-2016

Please cite this article as: J. Bastos-Arrieta, J. Muñoz, A. Stenbock-Fermor, M. Muñoz, D.N. Muraviev, F. Céspedes, L.A. Tsarkova, M. Baeza, Intermatrix Synthesis as a rapid, inexpensive and reproducible methodology for the *in situ* functionalization of nanostructured surfaces with Quantum Dots, *Applied Surface Science* (2016), http://dx.doi.org/10.1016/j.apsusc.2016.01.277

Intermatrix Synthesis as a rapid, inexpensive and reproducible methodology for the *in situ* functionalization of nanostructured surfaces with Quantum Dots

Julio Bastos-Arrieta*[1,2], Jose Muñoz[2,], Anja Stenbock-Fermor[3], Maria Muñoz[2], Dmitri N. Muraviev[2], Francisco Céspedes[2] Larisa A. Tsarkova[3] and Mireia Baeza[2]

[1]Department of Chemical Engineering, Universitat Politècnica de Catalunya, Av.Diagonal 647, 08028 Barcelona, Spain.

[2]Department of Chemistry, Universitat Autònoma de Barcelona, 08193, Barcelona, Spain

[3]DWI − Leibniz-Institut für Interaktive Materialien, Aachen 52056, Germany

*Corresponding Author: julio.bastos@upc.edu

JB: julio.bastos@upc.edu

JM: josemaria.munoz@uab.cat

AS: stenbock@dwi.rwth-aachen.de

MM: Maria.Munoz@uab.cat

DNM: Dimitri.Muraviev@uab.es

FC: francisco.cespedes@uab.cat

LT: tsarkova@dwi.rwth-aachen.de

MB: MariaDelMar.Baeza@uab.cat

Abstract

Intermatrix Synthesis (IMS) technique has proven to be a valid methodology for the *in situ* incorporation of quantum dots (QDs) in a wide range of nanostructured surfaces for the preparation of advanced hybrid-nanomaterials. In this sense, this communication reports the recent advances in the application of IMS for the synthesis of CdS-QDs with favourable distribution on sulfonated polyetherether ketone (SPEEK) membrane thin films (TFs), Multiwall Carbon Nanotubes (MWCNTs) and Nanodiamonds (NDs). The synthetic route takes advantage of the ion exchange functionality of the reactive surfaces for the loading of the QDs precursor and consequent QDs appearance by precipitation. The benefits of such modified nanomaterials were studied using CdS-QDs@MWCNTs hybrid-nanomaterials. CdS–QDs@MWCNTs has been used as conducting filler for the preparation of electrochemical nanocomposite sensors, which present electrocatalytic properties. Finally,

the optical properties of the QDs contained on MWCNTs could allow a new procedure for the analytical detection of nanostructured carbon allotropes in water.

Introduction

The progress in many fields of the modern technology within the last 20 years is determined by the rapid development and wide application of various nanomaterials (NMs) and nanocomposites on their base[1–4].

Regarding this fact, Metal Nanoparticles (MNPs) are objects of great interest in modern chemical research due to their special properties such as electrical, magnetic, optical and others, which are distinct from both those of the bulk material and those of isolated atoms and molecules[5].

However prior to their use, MNPs have to be stabilized. The stabilisation of MNPs is required for a number of reasons: 1) to prevent the uncontrollable growth of particles by preventing the nanoparticles aggregation; 2) to control the particles growth rate since if the rate is very low, their stability for a long time is assured; 3) to control particle size, and therefore, their special shape and the properties associated with it; and finally, 4) to enhance the particle solubility in various solvents what simplifies their handling and deposition on the materials surface. This stabilisation of MNPs can be achieved with the use polymeric supports and organic capping ligands[6–8].

The development of functional hybrid-nanomaterials combining different polymers and inorganic nanomaterials [9]-[10] as in polymer-metal nanocomposites (PMNCs), is one of the most promising solutions to the MNPs stability problem. Regarding this fact, Intermatrix Synthesis technique (IMS) is a simple, fast and low cost methodology for the synthesis of PMNCs. IMS is based on the ion exchange properties of the support resulting in the preparation of PMNCs[11–13]. This procedure coupled with Donnan Exclusion Effect (DEE) offers advantage in terms of MNPs distribution in the final added value material, where the MNPs are mainly located on the matrix surface due to the difficulty of the reducing agents to penetrate deeply into the supporting matrix as result of the electrostatic repulsion[14, 15].

The possibility of release of nanomaterials into the environment[16–20] results in the serious concerns about safety issues dealing with: 1) their higher toxicity in

comparison with their bulk counterparts; 2) the absence of the legislation normative for permitted levels of various NMs in water and air; and 3) the absence of the adequate analytical techniques for detection of NMs in the environment [21, 22].

Regarding this fact, it is essential to propose and to develop analytical methodologies for the quantification of nanomaterials, for example, in aqueous samples. This procedure could be based on the specific properties of the analyte under determination, such as for example Carbon Nanotubes (CNTs). However, they are known to be the most toxic carbon nanoallotrope. Nanodimonds (NDs) [23],[24, 25], which is other carbon nanoallotrope, exhibit interesting mechanical and optical properties, high surface areas and tuneable surface structures[25]. Moreover, they are non-toxic, which makes them suitable to biomedical applications, a feasible alternative as nanocarriers for addressed delivery of drugs and biolabeling[26],[27].

Despite their toxicity, CNTs find various applications since their discovery due to their structural properties, stability and high electrical and thermal conductivities. All these features make CNTs a valuable component of different kind of nanocomposites, which are used as a base for design of various devices such as, for example electrochemical (bio)sensors[28][29][30]. For this reason, the development of analytical techniques permitting their detection in the environment seems particularly important.

CNTs are known to be partially oxidized and as the result, bear on their surface the carboxylic functional groups. From this viewpoint, they can be considered as a “nano analogous” of fibrous carboxylic ion exchange materials such as, for example FIBAN K-4.[31, 32] The surface of these materials can be easily modified with MNPs as it has been shown in our recent publications[33,34].

Previous works related to decoration or modification of CNTs with nanocrystals such as MNPs usually involve thermal evaporation[35], electroless deposition by galvanic replacement[36], MNPs hydrosol absorption[37], electrochemical deposition[38]. These methods are mainly based on the use of high temperatures or organic solvents, involving a significant environmental impact of the process. There are green methodologies for the functionalization of CNTs with MNPs such as seed-mediated growth[39,40] in which metal salts solutions can be reduced by a strong reducing agent (e.g. $NaBH_4$) at room temperature

and aqueous solution. In addition; other green methodologies combine microwave radiation with polyol method for the synthesis of MNPs on CNTs for catalytic applications.[41–43]

Therefore, an analogous procedure can be used for modification of CNTs surface with easily detectable species, such as quantum dots (QDs). QDs are known to present quantum confinement effects during light excitation, which gives them interesting optical and semi-conducting properties. Tuning these features, and coupled them with its surface modification or using them for the surface modification of CNTs, led to explore the application of these nanocrystals in the field of sensors (fluorescent and biosensors) and to bioassays[44–47].

IMS has proved to be a valid procedure for the surface modification of polymeric ion exchange matrices such as resins, membranes and fibres with mono and bi-metallic MNPs. Depending on the chemical nature of these MNPs, the produced PMNCs have different applications: bactericide assays, complex water treatment, heterogeneous catalysis and electrocatalysis[5, 12, 33, 48–51]. In despite of the *in situ* formation of the MNPs on the polymeric support, its initial ion exchange properties are not significantly changed, which represents and advantage of IMS.

Sulfonated polyetherether ketone membrane (SPEEK) has a potential for proton exchange fuel cell applications.[52, 53] Due to its ion exchange properties, SPEEK has been widely used as polymeric matrix for the IMS of MNPs.[5, 48, 54] Consequently, preparing SPEEK polymeric thin films (PTFs) by spin coating (SC) offers a novel type of polymeric support for IMS. SC is currently a predominant technique used to produce uniform thin films of organic materials with customized thicknesses of the order of micrometres and nanometres[55],[56],[57]. MNPs applications depend on their distribution, as well as the density of MNPs over the support. As SPEEK is a well know matrix for IMS with a tuneable sulfonation degree and stability, it is interesting to look for the effects of SC in the final MNPs distribution, and making SC an alternative methodology for the preparation of MPNCs with well dispersed and distributed MNPs synthesized by IMS.

In this work we present the extended use of IMS for the preparation of CdS-QDs on novel reactive matrices such as CNTs, NDs and SPEEK/PTFs. This methodology includes two stages based on aqueous chemistry: 1) loading the functional groups with CdS-QDs precursor (e.g., metal complex ions) and 2) *in situ* formation of QDs in the supporting

matrix after precipitation of the precursor. Accordingly, the feasibility of CdS-QDs contained on MWCNTs (CdS-QDs@MWCNTs) for the preparation of epoxy nanocomposite electrodes was evaluated in terms of electrochemical and electroanalytical features. In addition, it is also proposed the use of IMS technique for the incorporation of CdS-QDs on carbon nanomaterials for the analytical detection of nanostructured carbon allotropes in water.

Experimental

Chemical and Reagents

Raw MWCNTs used in this research was provided by SES Research (Houston, TX, USA) whose physical properties are > 95% of carbon purity, 10–30 nm of outer diameter and has about 5–15 μm of length. It was produced using a chemical vapour deposition (CVD) method. Epotek H77A and its corresponding hardener Epotek H77B were obtained from Epoxy Technology (Billerica, MA, USA) and were used as polymeric matrix. CdS-QDs were synthesized using $Cd(NO_3)_2$ and Na_2S supplied by Sigma-Aldrich (St. Louis, MO, USA) and not required any farther treatment. The SPEEK precursor polymer (PEEK, Goodfellow) was also used without any pre-treatment.

All dissolutions were prepared using deionised water from a Milli-Q system (Millipore, Billerica, MA, USA). Potassium ferricyanide / ferrocyanide (99.8%), potassium chloride (99.5%), potassium phosphate dibasic anhydrous (> 99.0%) and potassium phosphate monobasic (>99.0%) and potassium hexacyanosferrate (II) trihydrate were purchased from Sigma-Aldrich (St. Louis, MO, USA). Finally, borom borohydride (96%) was provided by Panreac (Castellar del Vallès, Barcelona, Spain), and ion exchange resins were kindly supplied by Purolite® (Purolite Iberica S.I., Barcelona, Spain). All reagents were of the highest grade available and used without further purification.

Metal salts ($NaBH_4$, $CuSO_4 \cdot 5H_2O$ and others) from Sigma Aldrich were of p.a. grade were used as received.

NDs were kindly supplied by Dr. Andrey Yaroslavtsev and obtained by a synthetic methodology described somewhere else[25]. The detonation takes place in a closed chamber filled with an inert gas (dry synthesis) or iced water (wet synthesis) as coolant.

The product is a mixture of diamond particles 4–5 nm in diameter with other carbon allotropes and impurities.

Preparation of Matrices

a) SPEEK membrane synthesis and SC of PTFs:

Sulfonation of PEEK was carried out by following the procedure described elsewhere[5, 58] by using concentrated sulfuric acid at room temperature. The casting of SPEEK membranes was carried out from a 10% w/w solution of polymer in DMF by using a RK Paint Applicator (K Print Coat Instruments, Ltd.) coupled with temperature controller. The ion-exchange capacity (IEC) of SPEEK membrane was determined to be about 2 meq•g-1 SPEEK in all cases.

An exact amount of SPEEK membrane was dissolved in DMF. The result solution was sonicated for 10min, filtered through 1um filter and sonicated for 5 more minutes before SC.

Silica wafer supports were heated up to 200 ºC and cleaned with CO_2 (g). Then plasma etching was applied for 60 s for activating surface of the support and therefore provide more homogeneity of thin film coating.[59] Spin coater Laurell WS-650 was used for the preparation of SPEEK thin films. Previously, SPEEK solution was let to interact with the silica wafer support for around 10-15 s before starting SC for 2 min time at 2000 rpm. Thickness measurements of PTFs were made on an Omt - Optische Messtechnik Gmbh Ellipsometer.

b) NDs activation:

NDs were activated by 2.5 M nitric acid treatment with ultrasound for 2 h, with the consequent surface oxidation and appearance of carboxylic functionality which increases the ion exchange capacity of this support. A rinse procedure was carried out with MIliQ water and until pH=7. In addition, to obtain a more favourable ionic form of the NDs surfaces, NDs were immersed in alkaline 1.0 M NaCl solution (at pH≈10) with mechanical stirring to convert all carboxylic groups to Na^+ form.

c) MWCNTs:

MWCNTs were activated by 2.5 M nitric acid treatment with ultrasound for 2 h promoting the increase the ion exchange capacity of this support. The carboxylic groups on the

MWCNTs were converted to Na^+ form by their immersion 1.0 M NaCl solution with mechanical stirring.

Synthesis of CdS- QDs by IMS precipitation technique

The general procedure of synthesis was carried out by loading the raw multiwall carbon nanotubes functional groups with 20mL $Cd(NO_3)_2$ 0.1 M for 30 min. with magnetic stirring. MWCNTs were rinsed with deionized MiliQ water. Then 20 mL Na_2S 0.1 M were added to promote CdS-QDs precipitation on the surface of the MWCNTs, NDs and SPEEK-TFs. Finally, samples were rinsed once again with MiliQ water.

Electron Microscopy Characterisation

High Resolution Transmission Electron Microscopy (HR-TEM) images were obtained with the JEM-1400 unit with an acceleration voltage of 120kV. HR-(S)TEM (scanning – transmission electron microscope) images were taken with a FEI Tecnai G2 F20 S-TWIN HR-(S)TEM field emission of 200 kV with analytical EDS.

Sample preparation: Approximately 1 mg of sample was dispersed in 5 mL of acetone as organic solvent and then placed in ultrasound bath for one hour. Finally, a drop of the solution was placed on a grid and let it dry before TEM analysis. For SPEEK-PTFs analysis, the PTFs were dissolved in DMF and dropped on a grid.

Energy Dispersive X-Ray (EDS) microanalysis

HR-(S)TEM microscopy shows colour contrast depending on the composition of the sample. The clear zones present a higher weight composition. Combining this technique with EDS analysis, EDS spectra evidence composition differences as for the catalyst of the MWCNT and the CdS-QDs.

Metal content by thermogravimetric Analysis of CdS-QDs MWCNTs composites

Thermogravimetric analysis (TGA) were performed on a Netzsch instrument, model STA 449 F1 Jupiter®, with a flow of air. A ~20 mg sample was heated to 1000 ºC at 10 ºC/min, using flow of air. The mass of the sample was continuously measured as a function of temperature and the rate of weight loss (d.t.g.) was automatically recorded.

Voltammetric Experiments

All voltammograms were performed at room temperature (25 ºC) in a 10 mL glass cell (home-made), using a three-electrode configuration. Cyclic Voltammetry measurements were made in a 0.1 M KCl solution containing $6.5 \cdot 10^{-3}$ M $K_4[Fe(CN)_6]$ under quiescent condition (scan rate: 50 mV/s).

Electrochemical Performance of CdS-QDs@MWCNTs in epoxy nanocomposite electrodes

Regarding the feasibility for the preparation of epoxy composite electrodes with CdS-QDs on MWCNTs, the information of previous studies was taken into account considering that the optimal composition of the transducer material used for the construction of nanocomposite electrode was 10% of raw MWCNTs dispersed in epoxy Epotek H77 resin. Basing on our previously obtained results, 10% of conducting material content was considered as the optimum for MWCNTs/epoxy composite electrodes containing SES MWCNTs.(ref) This composition was also used in this work.

Confocal Microscopy

Samples were mounted on bottom-glass culture dishes (MatTek Corp., Ashland) and were examined using a TCS-SP5 (Leica Microsystems, Heidelberg, Germany) confocal laser scanning microscope located in Microscopy Facilities of Universitat Autònoma de Barcelona. Fluorescence Emission Spectra were obtained using a 63x objective with an excitation wavelength of 405 nm for all spectra. Recording data has a wavelength range from 425 nm to 775 nm with a band width of 10 nm and a spectral resolution of 7 nm. Raw MWCNTs do not present fluorescent emission signal.

Results and Discussion

Intermatrix Synthesis CdS-QDs in SPEEK Polymeric Thin Films (CdS-QDs@SPEEK/PTFs)

SPEEK membrane presents an ion exchange capacity (IEC) value of 2 meq•g^{-1} as product of the tuned sulfonation degree. This fact has made this polymeric membrane a suitable matrix for the implementation of IMS for the synthesis of different MNPs with different applications.[48, 60, 61]

Preparing PTFs of SPEEK membrane by SC involves the production of a material with optimal properties, which chemical properties are not changed. Consequently, the re-assembly and disposition of the functionality of the initial material make it suitable for IMS of Cd-QDs.

The formation of SPEEK/PTFs involves the equilibrium of several different species to produce the homogenous polymeric layer. The approach to achieve homogeneity in the layer thickness and distribution required several optimisation cycles of SPEEK polymer dissolved and dropped on a silicon wafer. The viscosity and surface tension of dissolved SPEEK, could cause non-homogenous film distribution, therefore a plasma etching[59] procedure was carried out on the silicon wafers to improve affinity between the wafer and the substrate as SPEEK flow on a flat spinning substrate is one of the most important physical processes involved in SC[56],[57].

SC of SPEEK involves different stages[57] 1) deposition of SPEEK on silicon wafer, 2) spin-up due to centrifuge force in which the substrate is accelerated up to is final desired rotation speed, 3) spin-off in which gradual fluid thinning occurs and 4) evaporation in which spin-off stage ends the film drying stage begins. Stages 1 to 3 are sequential. In addition, stages 3 and 4 usually overlap, being these two the more important for the final coating thickness

The election of the solvent is fundamental for homogenous coating. In this case, dimethyformamide (DMF) was selected because of the solubility of SPEEK in it and its volatility, favouring stages 3 and 4 of overall SC process. Thickness control during SC is dependent on the viscosity of the polymer drop to be coated (SPEEK) and its surface tension interaction with the wafer. This factor could be tuned by changing the concentration of SPEEK during deposition (1% to 5% v/v in DMF) and keeping constant the SC parameters such as time, revolutions and acceleration rate.

After obtaining different SPEEK/PTFs with different thicknesses (from 50 to 250 nm as obtained from ellipsometry measurements[62]) and considering that the ion exchange properties of SPEEK have not been significantly changed during preparation step, IMS of CdS-QDs can be carried out. The overall process can be described by equations 1 and 2. Firstly, from Na^+ form of SPEEK/PTF as the most favourable for the ion exchange. PTF is loaded with Cd^{2+} ions by a simple ionic exchange between cadmium and sodium ions,

equation (1). Equation (2) corresponds to the second stage of IMS, where the precipitation of CdS-QDs on the SPEEK/PTF is due to the addition of Na_2S. The regeneration of the initial Na^+ form of the support is achieved; which makes possible to repeat the overall cycle of IMS in order to increase the amount and thickness of the QDs synthesized[48, 60, 61].

$$2R\text{-}SO_3^- Na^+ + Cd^{2+} \rightarrow (R\text{-}SO_3^-)_2 Cd^{2+} + 2\ Na^+ \quad (1)$$

$$(R\text{-}SO_3^-)_2 Cd^{2+} + Na_2S \rightarrow 2R\text{-}SO_3^- Na^+ + CdS\downarrow \quad (2)$$

The surface modification of SPEEK/PTF is shown in Figure 1. Figure 1A shows a (S)TEM picture of CdS-QDs (white dots) and the Energy Dispersive X-Ray (EDS) of Figure 1B is a qualitative proof of the presence of the Cd and S; which would be expected to be located mainly on the surface regarding previous observation on SPEEK – NPs systems. [63]

The size distribution of the QDs on the SPEEK/PTF was determined of HR-TEM images (1C and 1D) from which a size distribution of (3.4 ± 0.3 nm) is obtained. Electron microscopy images and EDS analysis evidence that IMS is a valid technique for the synthesis of CdS-QDs in 2D polymeric supports such as SPEEK/PTFs prepared by SC. In addition, QDs size distribution was similar to other MNPs synthesized by IMS on SPEEK 3D films.[5]

Previous studies in similar systems of NPs and SPEEK [63], the location of the NPs is mainly on the surface as result of observation of cross section EDS analysis of the polymeric membrane. This is because of the coupling of the IMS with DEE and the abovementioned difficulty of the precipitation agent to penetrate the polymeric matrix as result of electrostatic equilibrium. In this case, IMS is coupled with DEE [15, 64, 65] predicts that the use of negatively charged precipitation agents as S^{2-} leads to the precipitation and location of the CdS -QDs mainly on the surface of the supporting matrix. Moreover, as seen in TEM image (1C), the stabilization offered by the polymeric support avoids the presence of agglomeration of QDs, as one additional advantage of IMS.

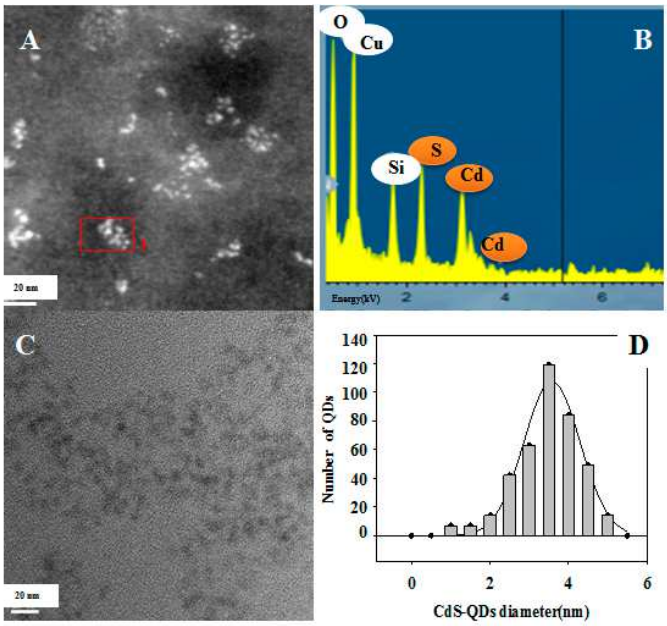

Figure 1: A) (S)TEM picture of CdS-QDs, indicating with a red square the analysed zone for the corresponding EDS on B. C) HR-TEM image and size distribution histogram of QDs (D).

Intermatrix Synthesis CdS-QDs in Nanodiamonds (CdS-QDs@NDs)

As stated before, NDs are less toxic nano carbon forms compared with MWCNTs. Their feasibility of applications due to their biocompatibility and high temperature resistant, make them an interesting matrix for the development of new low-dimensional carbon nanomaterials[25, 26, 66].

NDs usually present diameters from 4 to 5 nm and tend to agglomerate[25]. The experimental characterisation of raw NDs showed a size distribution value of 3.5 ± 0.3 nm. Agglomerates can be avoided by ultrasonication of the sample before TEM analysis (see Figure 2).

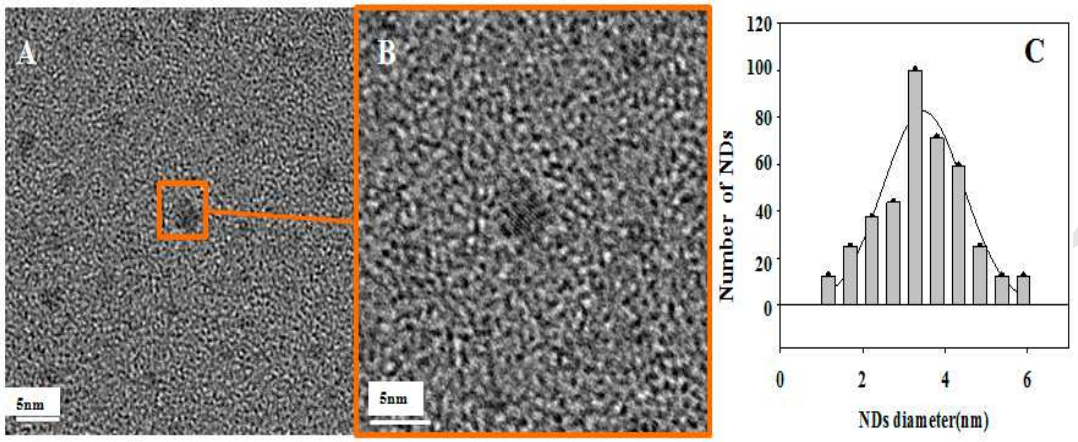

Figure 2: HR-TEM images of NDs (A, B magnification B>>>A) and raw NDs size distribution histogram(C).

The acidic treatment of the NDs leads to the appearance of carboxylic groups on their surface. Consequently, the activated NDs represent an analogous form of carboxylic polymers (eg. carboxylic resins and fibres) in which IMS was successfully applied for the preparation of MNPs.[34, 67]

IMS has never been used before for the surface modification of 0D supports as NDs. Even though; as it is based on the ion exchange functionality of the support; the IMS of CdS-QDs on NDs procedure proposed is described by equations (3) and (4).

$$2[\text{NDs-COO}^- \text{Na}^+] + \text{Cd}^{2+} \rightarrow [\text{NDs-COO}^-]_2 \text{Cd}^{2+} + 2\text{Na}^+ \quad (3)$$

$$[\text{NDs-COO}^-]_2 \text{Cd}^{2+} + \text{Na}_2\text{S} \rightarrow 2\,[\text{NDs-COO}^- \text{Na}^+] + \text{CdS}\downarrow \quad (4)$$

Equation (3) shows the Na^+ form of NDs. Sodium ion is exchanged by Cd^{2+} to complete the initial stage of IMS. Then, NDs sodium ion form is regenerated which makes feasible the repetition of IMS cycles, as can be seen in equation (4). In despite of this fact, it is important to highlight the size limitation of the reactive surface support (average 3.5 nm). The aim of the activation by acidic treatment is to increase the suitability of the NDs matrix (and MWCNTs) to the first loading stage of Intermatrix synthesis, which involves the ion exchange between the functional groups of the matrix with the QDs precursor (Cd^{2+} ion). In addition, the expected size of the CdS-QDs on these NDs supports is even smaller than the ones obtained on SPEEK/PTHs.

The presence of CdS-QDs on the NDs was evaluated and proved by HR-TEM pictures and EDS analysis (see Figure 3). The EDS spectra of raw NDs (Figure 3B) and modified-NDs with CdS-QDs (Figure 3D) were compared. The last spectrum verifies the presence of cadmium and sulphide.

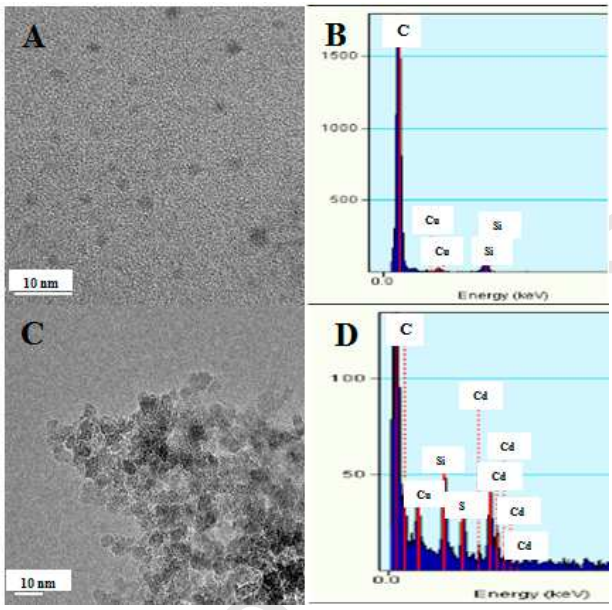

Figure 3: A) HR-TEM image of raw NDs and EDS spectra on B. C) HR- TEM image of CdS-QDs modified NDs and corresponding EDS spectra on D.

Intermatrix Synthesis of CdS-Qds in MWCNTs (CdS-QDs@MWCNTs)

The modification of reactive surfaces such as MWCNTs with QDs can be carried out by taking advantage of their ion exchange functionality. In this case, the first stage remains absolutely the same (loading the functional groups with NPs precursor), while the second one includes the formation of NPs (QDs) by precipitation reaction (instead of reduction). IMS can be described as follows: [11, 68]

Stage 1: Loading of Cd^{2+} ions (QDs precursors) onto the carboxylic groups of MWCNTs, equation (5), and

Stage 2: Precipitation of CdS-QDs on the MWCNTs surface by adding Na_2S solution, equation (6):

$$2[\text{MWCNTs-COO}^- \text{Na}^+] + Cd^{2+} \rightarrow [\text{MWCNTs-COO}^-]_2\, Cd^{2+} + 2Na^+ \quad (5)$$

$$[\text{MWCNTs-COO}^-]_2\, Cd^{2+} + Na_2S \rightarrow 2\,[\text{MWCNTs-COO}^- \text{Na}^+] + CdS\downarrow \quad (6)$$

As it is seen from equation (6), after carrying out the QDs formation reaction on the MWCNTs surface, the functional groups appear to be regenerated, as they are converted back into the Na^+ form. This means that the QDs formation cycle can be repeated again by using both equations without any additional pre-treatment of MWCNTs. This allows for accumulation of the desired amount of QDs on the surface of MWCNTs as seen in Figure 4.

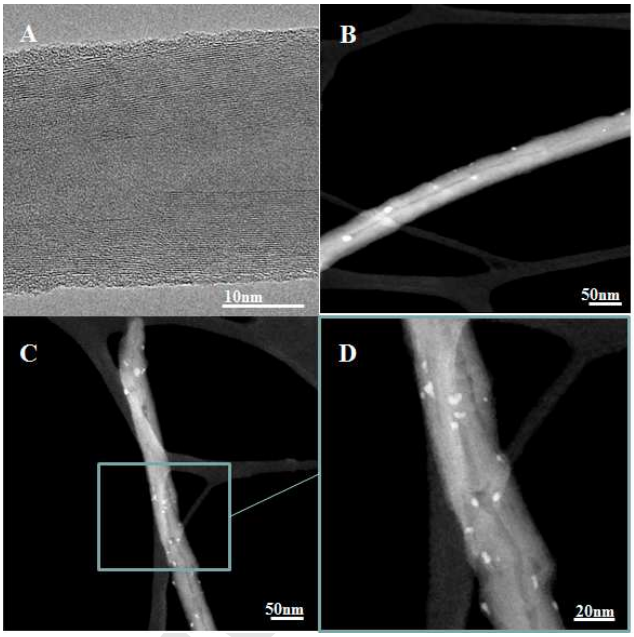

Figure 4: A) HR-TEM raw MWCNT B) HR-(S)TEM CdS-QDs on MWCNTs after one IMS cycle. C) and D) HR-(S)TEM images of CdS-QDs on MWCNTs after two sequential IMS cycles. Magnification of D>>C.

The microscopic characterisation of QD-MWCNTs nanocomposites shows in Figure 4B confirms that the CdS-QDs are located mainly on the surface of MWCNTs. Moreover, QDs are well separated from each other and do not form any visible agglomerates. The raw MWCNTs also contain Fe and Ni catalyst particles used by the manufacturer to grow the CNTs. These catalysts are located inside of the MWCNTs walls. In order to differentiate the QDs from the catalyst particles, EDS analysis of CdS-QDs@MWCNTs was also performed. Furthermore, the size distribution of the CdS-QDs is another parameter which can be used for their identification. An average diameter of CdS-QDs is 2.3 ± 0.4 nm as shown in Figure 5, while the one of the catalyst is higher (> 10 nm).

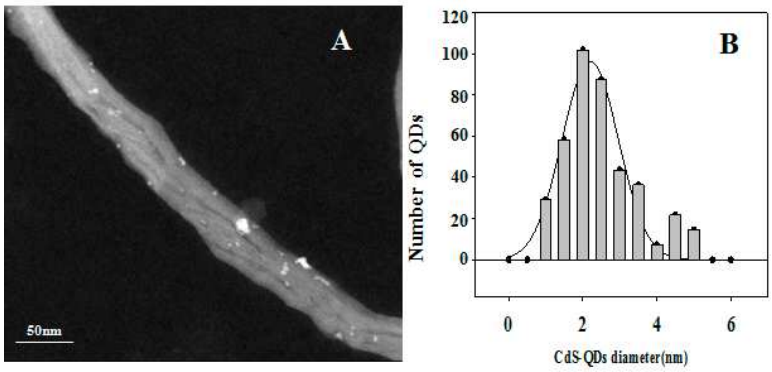

Figure 5: A) (S)TEM image and B) size distribution histogram for CdS-QDs on MWCNTs with an average diameter of 2.3 ± 0.4nm.

The corresponding EDS spectra in Figure 6 confirm the presence of CdS-QDs and clearly differentiate QDs from Ni catalyst. Signal of Cd content seems to be low due to the resolution of EDS technique for a single point analysis.

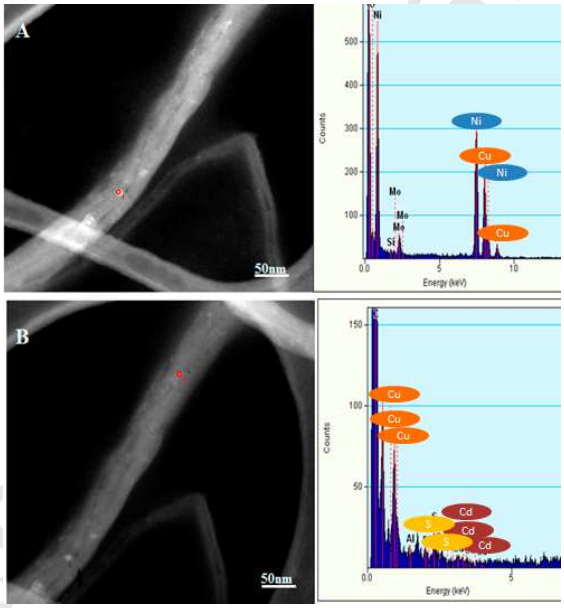

Figure 6: EDS spectra of A) MWNCTs Catalyst showing high Ni content. B) CdS-QDs showing the presence of Cd and S.

Thus, the QDs content was evaluated by the thermogravimetric analysis (TGA) and appeared to equal to 11.0% weight of CdS-QDs. As it is also seen in Figure 5, despite of a larger amount of QDs accumulated on the MWCNT surface after two sequential loading-precipitation cycles, no evidence of QD agglomerates formation can be detected for a 20.6% weight of CdS-QDs content. Therefore, this fact can be considered as an additional advantage of IMS as synthetic route.

Electrochemical characterization

CdS-QDs@MWCNTs/epoxy nanocomposite electrodes were constructed and electrochemically characterized by cyclic voltammetry (CV) in order to evaluate its feasibility as electrochemical sensors. In this context, the electrochemical performance of these electrodes were compared with the non-modified electrodes with CdS-QDs. Based on previous results, the MWCNT load for both kind of nanocomposite electrodes is 10% (w/w) [69–71]. Raw MWCNTs and CdS-QDs@MWCNTs were used as conducting materials for the construction of nanocomposite electrodes.

Figure 7 shows the typical cyclic voltammograms of the two kind of electrodes studied in this work (raw MWCNTs/epoxy and CdS-QDs@MWCNTs/epoxy nanocomposite electrodes) in $6.5 \cdot 10^{-3}$ M $[Fe(CN_6)]^{4-}$ containing 1.0 M KCl electrolytic solution at a scan rate of 50 $mV \cdot s^{-1}$. Different parameters such as peak height (I_p) and peak separation potential (ΔE) have been extracted from the cyclic voltammograms, see Table 1. The electroactive area can be calculated in terms of peak current (I_p, *A*) and scan rate (υ, $V \cdot s^{-1}$) according to the Randles-Sevčik equation:[72]

$$I_p = 3.01 \times 10^5 \cdot n^{3/2} (\alpha D_{red} \upsilon)^{1/2} A \cdot C^*_{red}$$

where n is number of electrons (n=1), C^*_{red} is the bulk concentration of the electroactive species (C^*_{red}= $6.5 \cdot 10^{-5}$ M), D_{red} corresponds to the diffusion coefficient of the reduced species (D_{red} = 6.32×10^{-6} $cm^2 \cdot s^{-1}$), α represents the charge transfer coefficient (α = 0.5) and υ represents the scan rate (υ = 0.01 $V \cdot s^{-1}$). According to these results, the electrode modified with CdS-QDs exhibited an enhancement of I_p around 56%, which was attributed to the increase of the electroactive area provided by modified-MWCNTs with CdS-QDs. This fact can be explained since QDs disperse the conductive microzones through the insulating polymeric matrix, obtaining electrodes more similar to a microelectrode array behaviour, with the benefits they present, such as higher signal-to-noise ratios and lower limits of detection [73]. Simultaneously, a change in ΔE was also observed (0.24 V *vs.* 0.41 V for CdS-QDs@MWCNTs/epoxy nanocomposite electrode), which can be explained due to the introduction of semi-conducting nanomaterials (CdS-QDs). This increase of ΔE turns into partial decrease in the system reversibility.[74] The enhancement of these electrochemical parameters resulted in an enhancement of several analytical parameters, as have been demonstrated recently [73].

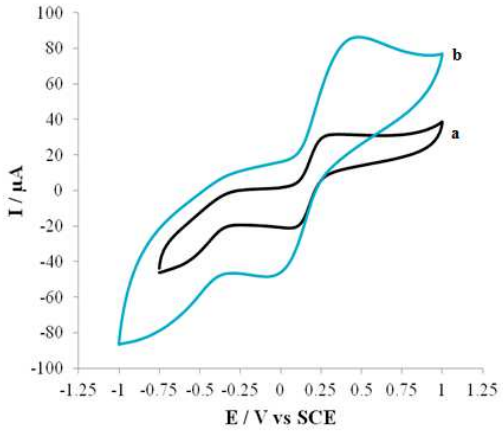

Figure 7: Cyclic voltammetry recorded in $6.5 \cdot 10^{-3}$ M $[Fe(CN)_6]^{4-}$ for electrodes containing a) raw MWCNTs and b) CdS-QDs@MWCNTs. Scan rate: 50 $mV \cdot s^{-1}$.

In order to verify if there is any release of CdS-QDs from MWCNTs to the media during the use of CdS-QDs modified-electrodes, different consecutive voltammograms were carried out, as is shown in Figure 8A. Four voltammograms were performed in 0.1 M KCl media, the first one without presence of Fe^{2+} and the following with increasing Fe^{2+} concentration. None peak was observed when the voltammogram was recorded without presence of Fe^{2+}, indicating that no redox reaction providing by the CdS-QDs takes place. These results demonstrate the stability of the CdS-QDs on the MWCNT surface and consequently in the nanocomposite electrode.

Then, the feasibility of this electrode in terms of electrochemical response and system reversibility was studied in front of different Fe^{2+} concentrations, as is also shown in Figure 8A. Peak current (anodic and cathodic) was directly proportional to $[Fe^{2+}]$ (Figure 8B and 8C). The linearity between peak current and $[Fe^{2+}]$ indicates the adequated system reversibility, obtaining a great regression of both, anodic peak current (I_{pa}) *vs.* $[Fe^{2+}]$ (r^2 = 0.9998; n=4) and cathodic peak current (I_{pc}) *vs.* $[Fe^{2+}]$ (r^2 = 0.9996; n=4).

The voltammetric results demonstrate a great electrochemical behaviour for CdS-QDs@MWCNTs/epoxy nanocomposite electrodes, opening the way to use this nanomaterials for the development of improved (bio)sensors from an electroanalytical point of view.

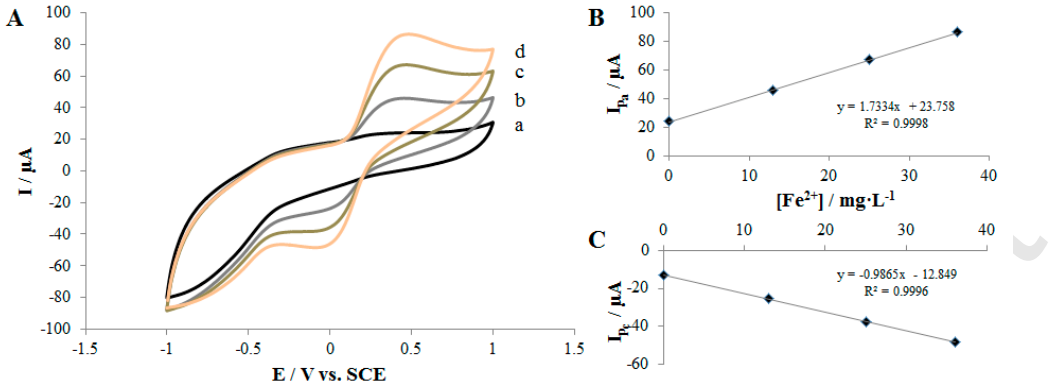

Figure 8: A) Cyclic voltammograms of CdS-QDs@MWCNTs/epoxy nanocomposite electrode a) in absence of Fe^{2+} and in presence of b) 13 ppm, c) 25 ppm and d) 37 ppm of Fe^{2+}. B) Lineal relationship between $[Fe^{2+}]$ and Ip_a and C) lineal relationship between $[Fe^{2+}]$ and Ip_c. The voltammograms were recorded at 50 mV·s^{-1}, using 0.1 M KCl as electrolytic solution.

Table 1. Electrochemical parameters obtained by CV in 0.1 M KCl containing $6.5 \cdot 10^{-3}$ M $[Fe(CN)_6]^{4-}$ at 50 mV·s^{-1} for the raw MWCNT/epoxy and CdS-QDs@MWCNTs/epoxy nanocomposite electrodes. A, I_p and ΔE parameters correspond to electroactive area, peak height and separation potential, respectively

Nanocomposite Electrode	A (cm^2)	I_p (mA)	ΔE (V)
Raw MWCNT/epoxy	0.05	0.021	0.24
CdS-QDs@MWCNTs/epoxy	0.11	0.048	0.41

Feasible application of CdS-QDs@MWCNTs for MWCNTs detection in water

After MWCNTs modification with CdS-QDs, they acquire optical properties, [75] demonstrating fluorescence emission spectra and start to be visible. These spectra were determined for different concentrations of CdS-QDs@MWCNTs in aqueous solution. Figure 9 presents the schematic diagram of sample preparation procedure for proposed analytical methodology for detection of CNTs in water.

The procedure is based on the hypothesis that CdS-QDs can be formed only on the surface of supporting material, such as for example MWCNTs. The surface of this material serves as both QDs formation medium as it bears the QDs-precursors (Cd^{2+} ions fixed on the carboxylic groups of CNTs) and the QDs-stabilizing medium as it prevents their agglomeration and uncontrollable grows (see Figure 5). Based on this hypothesis, it was also assumed that QDs cannot be formed in the QDs-free aqueous phase (used as blank) as in this case only the formation of CdS macro crystalline precipitate can occur.

Precipitation of CdS in blank was carried out by using the same reagent amount as for IMS of CdS-QDs on MWCNTs.

Then, the solution obtained was centrifuged. The aliquot of the resulting upper liquid phase was used as blank solution. An analogous procedure was applied for the water samples containing MWCNTs. After centrifugation, aliquots from the samples containing different MWCNTs concentration (differing by factors 1x, 2x and 3x) were taken for spectrophotometric analysis.

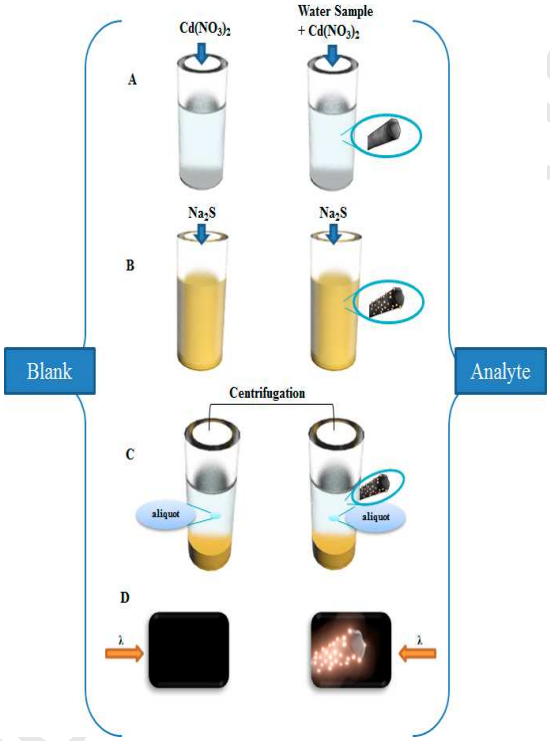

Figure 9: Scheme of analytical procedure for determination of MWCNTs in water. A) addition of $Cd(NO_3)_2$ aqueous solution to blank and water sample under analysis, B) precipitation of $CdS_{(s)}$ and formation of CdS-QDs on MWCNTs surface, C) centrifugation and D) aliquot from liquid phases of blank and analyte is analysed on spectrophotometer for detection of MWCNTs due to presence of CdS-QDs.

Figure 10 presents the values of fluorescent emission at the wavelength of λ= 405nm for three different concentrations of CdS-QDs@MWCNTs (obtained after one QDs loading cycle) in aqueous phase. As it is seen in Figure 9, the fluorescent emission at this particular wavelength appears to be directly proportional to the concentration of analyte (MWCNTs) in the sample. This fact can be used for the quantitative detection of MWCNTs in water samples, considering a suspension of raw MWCNTs as blank sample (no fluorescence emission is observed as shown in figure 10).

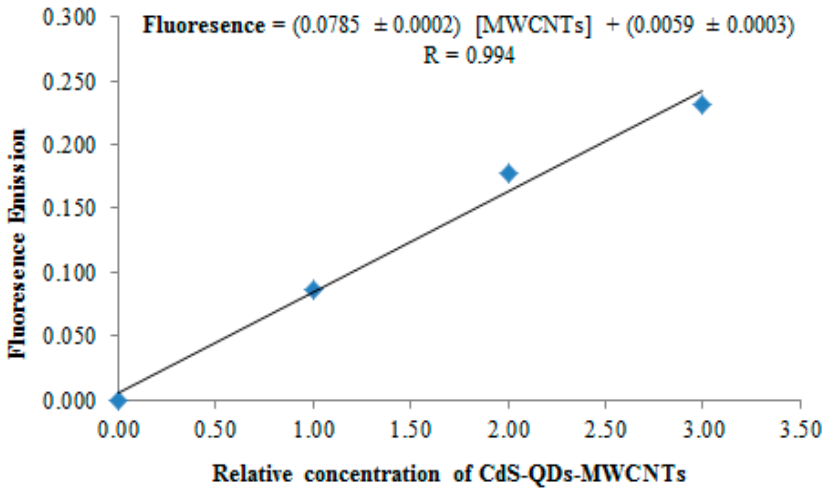

Figure 10: Dependence of intensity of fluorescence emission at wavelength of λ= 405nm on relative concentration of MWCNTs decorated with CdS-QDs. Zero point corresponds to emission of blank (see text).

Consequently, it can be concluded that non-aggressive IMS technique proves to be applicable for the functionalization of MWCNTs with CdS-QDs what makes them spectrophotometrically detectable. IMS methodology is a simple technique as the amount of regents used for IMS of QDs on MWCNTs surface can be minimized and only aqueous solutions are used in all cases. In addition, it seems important to emphasise that this methodology offers the possibility of detection of these NMs by using simple procedure shown in Figure 9, what makes detectable its presence in water.

An increase of CdS-QDs load on MWCNTs surface combined with more sensitive spectrophotometric equipment, will allow to substantially decreasing the limit of detection of MWCNTs in water.

Moreover, the procedure seems to be easily adaptable for detection of other carbon NMs such fullerenes, NDs and some others. Moreover, the final distribution of the QDs on the support makes feasible the application of the obtained NMs also in catalysis or electrocatalysis. The aim of the acidic treatment is to increase the suitability of the reactive matrix (in this case MWCNTs and NDs) to the first loading stage of Intermatrix synthesis, which involves the ion exchange between the functional groups of the matrix with the QDs precursor, Cd^{2+} ion. The increase of the suitability of the reactive matrix (CNTS, NDs or other carbon nano –allotropes) by this treatment will be reflected in the consequent increase

of the sensitivity of the detection methodology. In this case, the detection occurs due to the fluorescent features of the *CdS-QDs*, which will remain the same independently of the support where they can be synthesized. Regarding this, in despite of the activation or not of the support by the acidic treatment, the synthesis of the CdS-QDs is still feasible and therefore the application of the detection methodology.

This proposed methodology has the assumption that the formation of the QDs is only on the surface of the MWCNTs. In the absence of this support, CdS forms conventional macroscopic scale precipitate which can be easily separated by centrifugation. Meanwhile, at the same centrifugation conditions the CdS-QDs@MWCNTs will still remain suspended in aqueous phase.

Conclusions

IMS demonstrates to be a valid route for the systematically preparation of multi-dimensional nanocomposite materials (from 0 D such as NDs to 3 D as granulated exchange polymers) by the modification of different types of reactive surfaces with CdS–QDs.

In addition, IMS is a non-aggressive, simple and inexpensive technique, applicable for the functionalisation of MWCNTs, NDs and PTFs with CdS-QDs with favourable distribution as shown in electron microscopy characterisation.

MWCNTs were chosen as carbon nanomaterial to verify the feasibility of these modified-carbon materials with CdS-QDs, in terms of electrochemical and fluorescent properties.

On the one hand, the electrochemical response of CdS-QDs@MWCNTs/epoxy nanocomposite electrodes was evaluated by CV and compared with the non-modified electrode. A significant enhancement of the I_p was observed for the CdS-QDs modified-electrode, which was 65% higher than the non-modified electrode. This electrochemical enhancement makes them interesting materials in the (bio)sensor field due to their proved electrocatalytical properties. Furthermore, voltammetric experiments were conclusive in terms of stability of CdS-QDs on the MWCNT surface, as no redox reactions of Cd^{2+} and S^{2-} were observed.

On the other hand, taking into account the proposed hypothesis of the preferential formation of CdS-QDs on the MWCNTs surface, it was demonstrated that after

modification with QDs the intensity of fluorescent emission at a certain wavelength (λ= 405 nm) appears to be directly proportional to the CNTs concentration in water. This can be used for the detection of CNTs in water samples. Thus, a simple analytical procedure based on the above hypothesis for the detection of MWCNTs in water has been proposed and experimentally prove.

Finally, the IMS technique has been shown to be applicable for the synthesis of CdS–QDs on MWCNTs by precipitation route, what results to the favourable distribution of QDs on the surface of the nanotubes. The functional groups of the MWCNTs are converted back into the initial ionic form (regenerated) after the CdS precipitation stage, what permits to carry out several sequential metal-loading-precipitation cycles to increase the QDs content in the final nanocomposite material.

Acknowledgements

Programa Operatiu de Catalunya (FEDER) is acknowledged for the financial support within the project VALTEC09-02-0058. JB and JM also thank Universitat Autònoma de Barcelona for the personal grants during their Ph.D. Studies. Also Servei de Microscòpia of the Universitat Autònoma de Barcelona is also acknowledged for the electron microscopy images. Dr. Andrey Yaroslavtsev is specially acknowledged for supplying the raw NDs samples.

References:

1. Xu P, Han X, Zhang B, et al. (2014) Multifunctional polymer-metal nanocomposites via direct chemical reduction by conjugated polymers. Chem Soc Rev 43:1349–60. doi: 10.1039/c3cs60380f
2. Hussain F (2006) Review article: Polymer-matrix Nanocomposites, Processing, Manufacturing, and Application: An Overview. J Compos Mater 40:1511–1575. doi: 10.1177/0021998306067321
3. Paul DR, Robeson LM (2008) Polymer nanotechnology: Nanocomposites. Polymer (Guildf) 49:3187–3204. doi: 10.1016/j.polymer.2008.04.017
4. Kao J, Thorkelsson K, Bai P, et al. (2013) Toward functional nanocomposites: taking the best of nanoparticles, polymers, and small molecules. Chem Soc Rev 42:2654–78. doi: 10.1039/c2cs35375j
5. Ruiz P, Muñoz M, Macanás J, Muraviev DN (2010) Intermatrix Synthesis of Polymer−Copper Nanocomposites with Tunable Parameters by Using Copper

Comproportionation Reaction. Chem Mater 22:6616–6623. doi: 10.1021/cm102122c

6. Corbierre MK, Cameron NS, Sutton M, et al. (2001) Polymer-stabilized gold nanoparticles and their incorporation into polymer matrices. J Am Chem Soc 123:10411–2.

7. Wojczykowski K, Meissner D, Jutzi P, et al. (2006) Reliable stabilization and functionalization of nanoparticles through tridentate thiolate ligands. Chem Commun (Camb) 3693–5. doi: 10.1039/b606360h

8. Harris L a., Goff JD, Carmichael a. Y, et al. (2003) Magnetite nanoparticle dispersions stabilized with triblock copolymers. Chem Mater 15:1367–1377. doi: 10.1021/cm020994n

9. Gómez-Romero P, Ayyad O, Suárez-Guevara J, Muñoz-Rojas D (2010) Hybrid organic–inorganic materials: from child's play to energy applications. J Solid State Electrochem 14:1939–1945. doi: 10.1007/s10008-010-1076-y

10. Mehdi A, Reye C, Corriu R (2011) From molecular chemistry to hybrid nanomaterials. Design and functionalization. Chem Soc Rev 40:563–74. doi: 10.1039/b920516k

11. Ruiz P, Macanás J, Muñoz M, Muraviev DN (2011) Intermatrix synthesis: easy technique permitting preparation of polymer-stabilized nanoparticles with desired composition and structure. Nanoscale Res Lett 6:343. doi: 10.1186/1556-276X-6-343

12. Alonso A, Muñoz-Berbel X, Vigués N, et al. (2012) Intermatrix synthesis of monometallic and magnetic metal/metal oxide nanoparticles with bactericidal activity on anionic exchange polymers. RSC Adv 2:4596–4599. doi: 10.1039/c2ra20216f

13. Bastos-Arrieta J, Shafir A, Alonso A, et al. (2012) Donnan exclusion driven intermatrix synthesis of reusable polymer stabilized palladium nanocatalysts. Catal Today 193:207–212. doi: 10.1016/j.cattod.2012.01.002

14. Sarkar S, Sengupta AK, Prakash P (2010) The Donnan membrane principle: opportunities for sustainable engineered processes and materials. Environ Sci Technol 44:1161–6. doi: 10.1021/es9024029

15. Levenstein R, Hasson D, Semiat R (1996) Utilization of the Donnan effect for improving electrolyte separation with nanofiltration membranes. J Memb Sci 116:77–92.

16. Hansen SF, Carlsen L, Tickner J a. (2007) Chemicals regulation and precaution: does REACH really incorporate the precautionary principle. Environ Sci Policy 10:395–404. doi: 10.1016/j.envsci.2007.01.001

17. Nijhara R, Balakrishnan K (2006) Bringing nanomedicines to market: regulatory challenges, opportunities, and uncertainties. Nanomedicine 2:127–36. doi: 10.1016/j.nano.2006.04.005

18. Milburn C (2012) Greener on the Other Side: Science Fiction and the Problem of

Green Nanotechnology. Configurations 20:53–87. doi: 10.1353/con.2012.0008

19. Pacheco-Torgal F, Jalali S (2011) Nanotechnology: Advantages and drawbacks in the field of construction and building materials. Constr Build Mater 25:582–590. doi: 10.1016/j.conbuildmat.2010.07.009

20. Lee KJ, Nallathamby PD, Browning LM, et al. (2007) In vivo imaging of transport and biocompatibility of single silver nanoparticles in early development of zebrafish embryos. ACS Nano 1:133–43. doi: 10.1021/nn700048y

21. Robison WL (2011) Nano-Technology, Ethics, and Risks. Nanoethics 5:1–13. doi: 10.1007/s11569-010-0108-5

22. Franco A, Hansen SF, Olsen SI, Butti L (2007) Limits and prospects of the "incremental approach" and the European legislation on the management of risks related to nanomaterials. Regul Toxicol Pharmacol 48:171–83. doi: 10.1016/j.yrtph.2007.03.007

23. Sharifi S, Behzadi S, Laurent S, et al. (2012) Toxicity of nanomaterials. Chem Soc Rev 41:2323–43. doi: 10.1039/c1cs15188f

24. Biolabeling N, Ho D (2009) Beyond the Sparkle□: The Impact of. 3:3825–3829.

25. Mochalin VN, Shenderova O, Ho D, Gogotsi Y (2011) The properties and applications of nanodiamonds. Nat Nanotechnol 7:11–23. doi: 10.1038/nnano.2011.209

26. Purtov K V, Petunin a I, Burov a E, et al. (2010) Nanodiamonds as Carriers for Address Delivery of Biologically Active Substances. Nanoscale Res Lett 5:631–636. doi: 10.1007/s11671-010-9526-0

27. Khabashesku VN, Margrave JL, Barrera EV (2005) Functionalized carbon nanotubes and nanodiamonds for engineering and biomedical applications. Diam Relat Mater 14:859–866. doi: 10.1016/j.diamond.2004.11.006

28. Gao C, Li W, Morimoto H, et al. (2006) Magnetic carbon nanotubes: synthesis by electrostatic self-assembly approach and application in biomanipulations. J Phys Chem B 110:7213–20. doi: 10.1021/jp0602474

29. Wang D, Li Z-C, Chen L (2006) Templated synthesis of single-walled carbon nanotube and metal nanoparticle assemblies in solution. J Am Chem Soc 128:15078–9. doi: 10.1021/ja066617j

30. Balasubramanian K, Burghard M (2005) Chemically functionalized carbon nanotubes. Small 1:180–92. doi: 10.1002/smll.200400118

31. Sarkar S, Guibal E, Quignard F, SenGupta a. K (2012) Polymer-supported metals and metal oxide nanoparticles: synthesis, characterization, and applications. J Nanoparticle Res 14:715. doi: 10.1007/s11051-011-0715-2

32. Greenleaf JE, Lin J, Sengupta AK (2006) Two novel applications of ion exchange fibers: Arsenic removal and chemical-free softening of hard water. Environ Prog 25:300–311. doi: 10.1002/ep.10163

33. Alonso A, Vigués N, Muñoz-Berbel X, et al. (2011) Environmentally-safe bimetallic Ag@Co magnetic nanocomposites with antimicrobial activity. Chem Commun (Camb) 47:10464–6. doi: 10.1039/c1cc13696h

34. Alonso A, Macanás J, Shafir A, et al. (2010) Donnan-exclusion-driven distribution of catalytic ferromagnetic nanoparticles synthesized in polymeric fibers. Dalton Trans 39:2579–86. doi: 10.1039/b917970d

35. Bittencourt C, Felten a., Ghijsen J, et al. (2007) Decorating carbon nanotubes with nickel nanoparticles. Chem Phys Lett 436:368–372. doi: 10.1016/j.cplett.2007.01.065

36. Choi HC, Shim M, Bangsaruntip S, Dai H (2002) Spontaneous reduction of metal ions on the sidewalls of carbon nanotubes. J Am Chem Soc 124:9058–9.

37. Lee KY, Kim M, Hahn J, et al. (2006) Assembly of metal nanoparticle-carbon nanotube composite materials at the liquid/liquid interface. Langmuir 22:1817–21. doi: 10.1021/la052435b

38. Qu L, Dai L (2005) Substrate-enhanced electroless deposition of metal nanoparticles on carbon nanotubes. J Am Chem Soc 127:10806–7. doi: 10.1021/ja053479+

39. Murphy CJ, Jana NR (2002) Controlling the Aspect Ratio of Inorganic Nanorods and Nanowires. Adv Mater 14:80–82. doi: 10.1002/1521-4095(20020104)14:1<80::AID-ADMA80>3.0.CO;2-#

40. Nikoobakht B, El-Sayed M (2003) Preparation and growth mechanism of gold nanorods (NRs) using seed-mediated growth method. Chem Mater 1957–1962.

41. Guo Z, Chen Y, Li L, et al. (2010) Carbon nanotube-supported Pt-based bimetallic catalysts prepared by a microwave-assisted polyol reduction method and their catalytic applications in the selective hydrogenation. J Catal 276:314–326. doi: 10.1016/j.jcat.2010.09.021

42. Wildgoose GG, Banks CE, Compton RG (2006) Metal nanoparticles and related materials supported on carbon nanotubes: methods and applications. Small 2:182–93. doi: 10.1002/smll.200500324

43. Liu X, Zeng P, Peng T, et al. (2012) Preparation of multiwalled carbon nanotubes/Cd0.8Zn0.2S nanocomposite and its photocatalytic hydrogen production under visible-light. Int J Hydrogen Energy 37:1375–1384. doi: 10.1016/j.ijhydene.2011.10.030

44. Elliott SD, Moloney MP, Gun'ko YK (2008) Chiral shells and achiral cores in CdS quantum dots. Nano Lett 8:2452–7. doi: 10.1021/nl801453g

45. Petryayeva E, Algar WR, Medintz IL (2013) Quantum dots in bioanalysis: a review of applications across various platforms for fluorescence spectroscopy and imaging. Appl Spectrosc 67:215–52. doi: 10.1366/12-06948

46. Moloney MP, Gun'ko YK, Kelly JM (2007) Chiral highly luminescent CdS quantum dots. Chem Commun (Camb) 7345:3900–2. doi: 10.1039/b704636g

47. Bera D, Qian L, Tseng T-K, Holloway PH (2010) Quantum Dots and Their

Multimodal Applications: A Review. Materials (Basel) 3:2260–2345. doi: 10.3390/ma3042260

48. Ruiz P, Muñoz M, Macanás J, et al. (2010) Intermatrix synthesis of polymer stabilized inorganic nanocatalyst with maximum accessibility for reactants. Dalton Trans 39:1751–7. doi: 10.1039/b917929a

49. Alonso A, Bastos-arrieta J, Davies GL, et al. Ecologically Friendly Polymer-Metal and Polymer- Metal Oxide Nanocomposites for Complex Water Treatment.

50. Domènech B, Muñoz M, Muraviev DN, Macanás J (2011) Polymer-stabilized palladium nanoparticles for catalytic membranes: ad hoc polymer fabrication. Nanoscale Res Lett 6:406. doi: 10.1186/1556-276X-6-406

51. Domènech B, Muñoz M, Muraviev DN, Macanás J (2014) Uncommon patterns in Nafion films loaded with silver nanoparticles. Chem Commun (Camb) 50:4693–5. doi: 10.1039/c4cc01285b

52. Erdener H, Akay RG, Yücel H, et al. (2009) Effects of sulfonated polyether-etherketone (SPEEK) and composite membranes on the proton exchange membrane fuel cell (PEMFC) performance. Int J Hydrogen Energy 34:4645–4652. doi: 10.1016/j.ijhydene.2008.08.066

53. Zhang H, Li X, Zhao C, et al. (2008) Composite membranes based on highly sulfonated PEEK and PBI□: Morphology characteristics and performance. 308:66–74. doi: 10.1016/j.memsci.2007.09.045

54. Muraviev DN, Ruiz P, Muñoz M, Macanás J (2008) Novel strategies for preparation and characterization of functional polymer-metal nanocomposites for electrochemical applications. Pure Appl Chem 80:2425–2437. doi: 10.1351/pac200880112425

55. Chou K-S, Huang K-C, Lee H-H (2005) Fabrication and sintering effect on the morphologies and conductivity of nano-Ag particle films by the spin coating method. Nanotechnology 16:779–784. doi: 10.1088/0957-4484/16/6/027

56. Decher G, Schlenoff JB (2012) Multilayer Thin Films. doi: 10.1002/9783527646746

57. Sahu N, Parija B, Panigrahi S (2009) Fundamental understanding and modeling of spin coating process: A review. Indian J Phys 83:493–502. doi: 10.1007/s12648-009-0009-z

58. Anderson HR, Kopitzkei RW, Linkous CA (1998) DEVELOPMENT ELECTROLYTES OF NEW PROTON EXCHANGE FOR WATER ELECTROLYSIS TEMPERATURES MEMBRANE AT HIGHER. 23:525–529.

59. Höcker H (2002) Plasma treatment of textile fibers. Pure Appl Chem 74:423–427.

60. Muraviev DN, Macanás J, Ruiz P, et al. (2008) Synthesis, stability and electrocatalytic activity of polymer-stabilized monometallic Pt and bimetallic Pt/Cu core-shell nanoparticles. Phys Status Solidi Appl Mater Sci 205:1460–1464. doi: 10.1002/pssa.200778132

61. Muraviev D, Macanas J, Farre M, et al. (2006) Novel routes for inter-matrix

synthesis and characterization of polymer stabilized metal nanoparticles for molecular recognition devices. Sensors Actuators B Chem 118:408–417. doi: 10.1016/j.snb.2006.04.047

62. Redel E, Mirtchev P, Huai C, et al. (2011) Nanoparticle films and photonic crystal multilayers from colloidally stable, size-controllable zinc and iron oxide nanoparticles. ACS Nano 5:2861–9. doi: 10.1021/nn103464r

63. Ruiz P, Muñoz M, Macanás J, Muraviev DN (2010) Intermatrix Synthesis of Polymer−Copper Nanocomposites with Tunable Parameters by Using Copper Comproportionation Reaction. Chem Mater 22:6616–6623. doi: 10.1021/cm102122c

64. Donnan FG (1995) Theory of membrane equilibria and membrane potentials in the presence of non-dialysing electrolytes. A contribution to physical-chemical physiology. J Memb Sci 100:45–55. doi: 10.1016/0376-7388(94)00297-C

65. Mijangos F, Tikhonov N, Ortueta M, Dautov A (2002) Modeling Ion-Exchange Kinetics in Bimetallic Systems. Ind Eng Chem Res 41:1357–1363. doi: 10.1021/ie010317n

66. Fu C-C, Lee H-Y, Chen K, et al. (2007) Characterization and application of single fluorescent nanodiamonds as cellular biomarkers. Proc Natl Acad Sci U S A 104:727–32. doi: 10.1073/pnas.0605409104

67. Alonso A, Muñoz-Berbel X, Vigués N, et al. (2012) Characterization of fibrous polymer silver/cobalt nanocomposite with enhanced bactericide activity. Langmuir 28:783–90. doi: 10.1021/la203239d

68. Muraviev DN (2005) Inter-matrix synthesis of polymer stabilised metal nanoparticles for sensor applications. Contrib to Sci 3:19–32.

69. Olivé-Monllau R, Martínez-Cisneros CS, Bartrolí J, et al. (2011) Integration of a sensitive carbon nanotube composite electrode in a ceramic microanalyzer for the amperometric determination of free chlorine. Sensors Actuators, B Chem 151:416–422. doi: 10.1016/j.snb.2010.10.017

70. Olivé-Monllau R, Baeza M, Bartrolí J, Céspedes F (2009) Novel Amperometric Sensor Based on Rigid Near-Percolation Composite. Electroanalysis 21:931–938. doi: 10.1002/elan.200804494

71. Olivé-Monllau R, Esplandiu MJ, Bartrolí J, et al. (2010) Strategies for the optimization of carbon nanotube/polymer ratio in composite materials: Applications as voltammetric sensors. Sensors Actuators B Chem 146:353–360. doi: 10.1016/j.snb.2010.02.017

72. Laoire CO, Mukerjee S, Abraham KM, et al. (2009) Elucidating the mechanism of oxygen reduction for lithium-air battery applications. J Phys Chem C 113:20127–20134. doi: 10.1021/jp908090s

73. Muñoz J, Bastos-Arrieta J, Muñoz M, et al. (2015) CdS quantum dots as a scattering nanomaterial of carbon nanotubes in polymeric nanocomposite sensors for microelectrode array behavior. J Mater Sci. doi: 10.1007/s10853-015-9484-0

74. Wang J (2006) Analytical Electrochemistry, Third Edition. Anal Electrochem Third Ed. doi: 10.1002/0471790303

75. Son JS, Park K, Kwon SG, et al. (2012) Dimension-controlled synthesis of CdS nanocrystals: from 0D quantum dots to 2D nanoplates. Small 8:2394–402. doi: 10.1002/smll.201200506

Highlights:

- Nanodiamond functionalization with CdS quantum dots
- Approach for Carbon Nanotube detection in water samples.
- Simple Functionalization of thin polymeric nanolayers with quantum dots

*Graphical Abstract (for review)

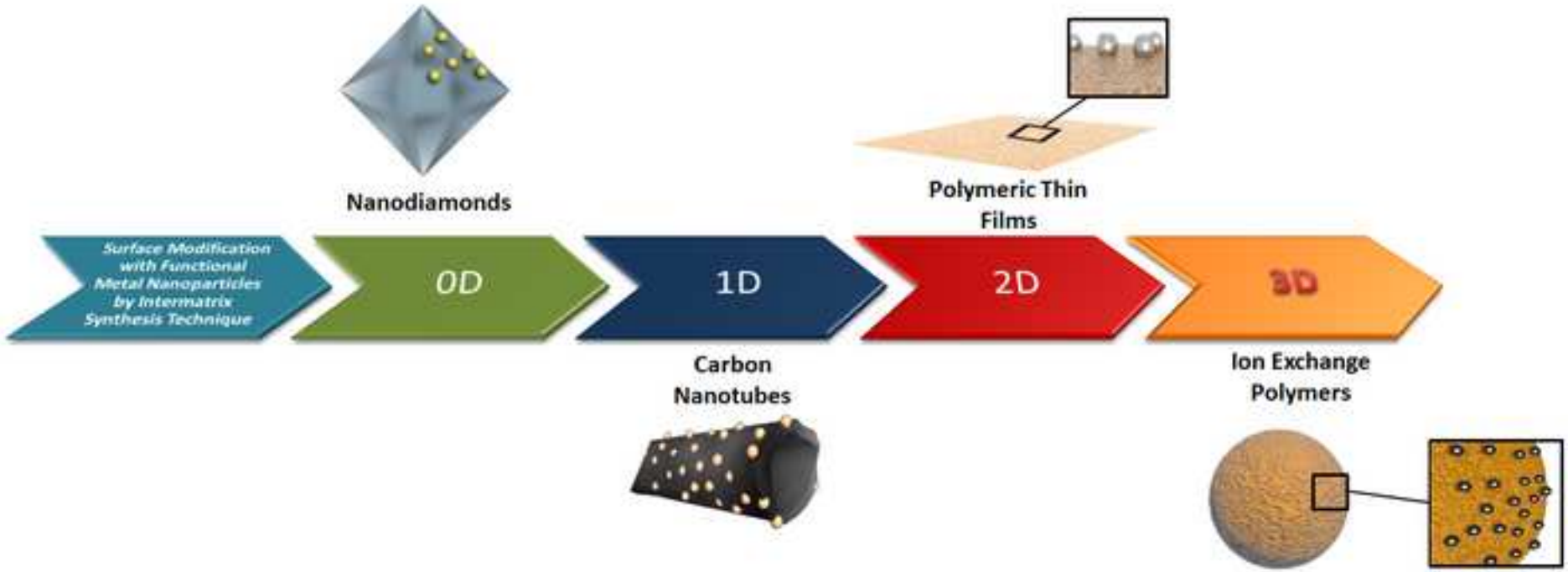

Figure 1

Click here to download high resolution image

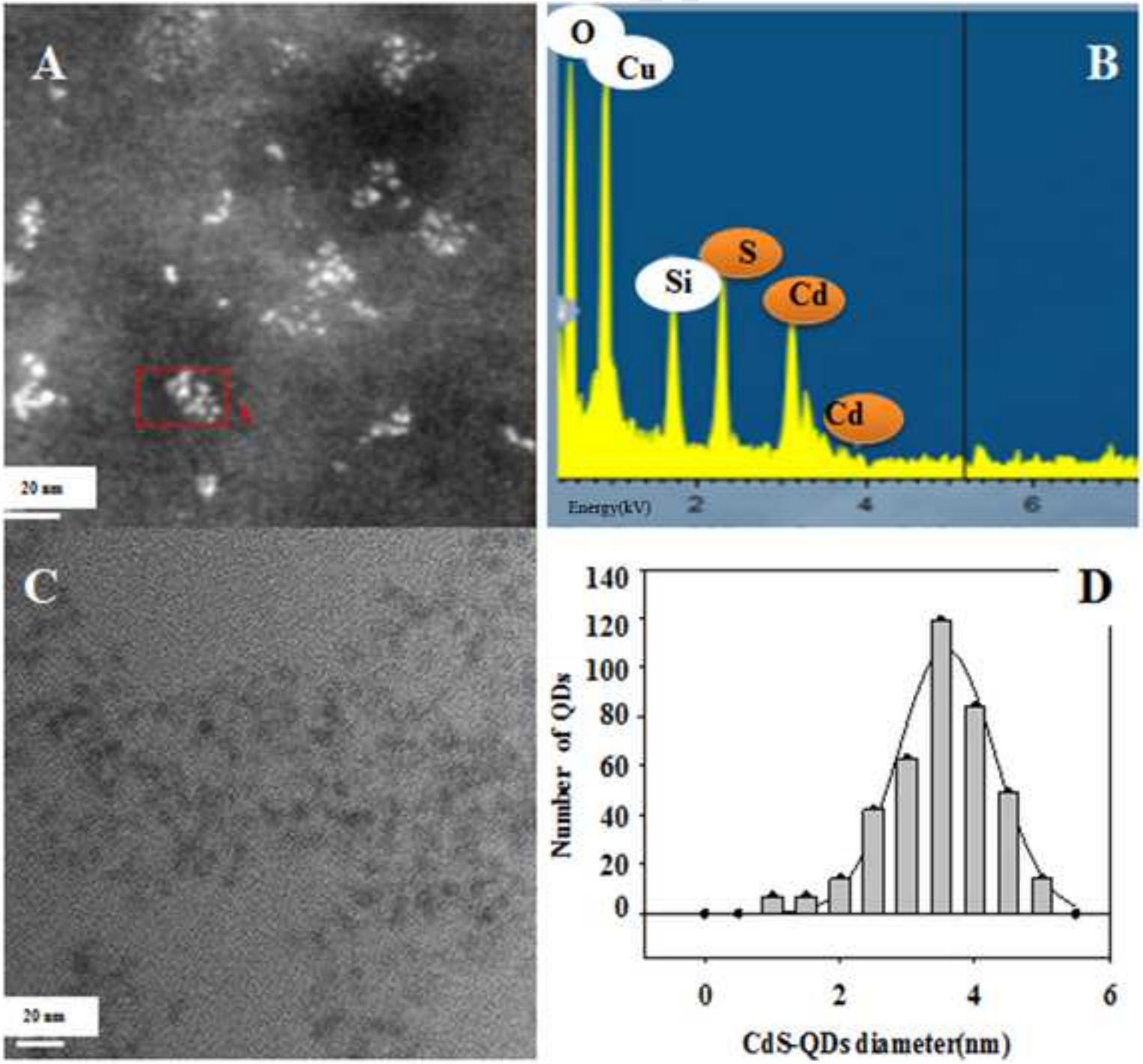

Figure 2

Click here to download high resolution image

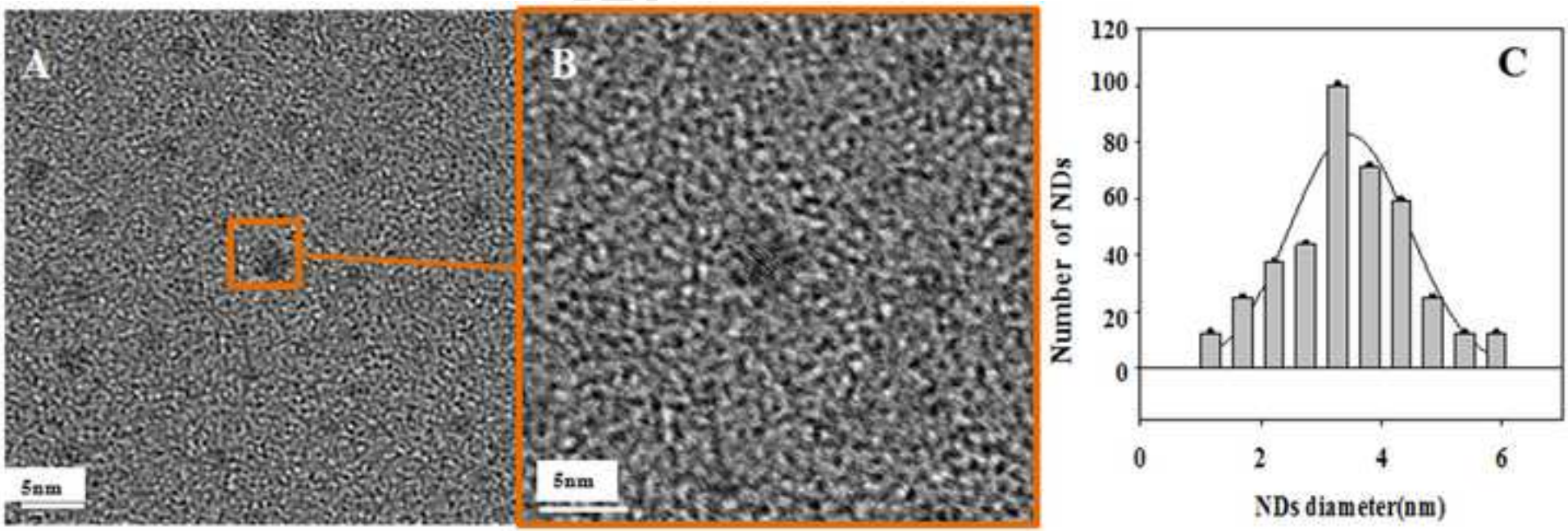

Figure 3

Click here to download high resolution image

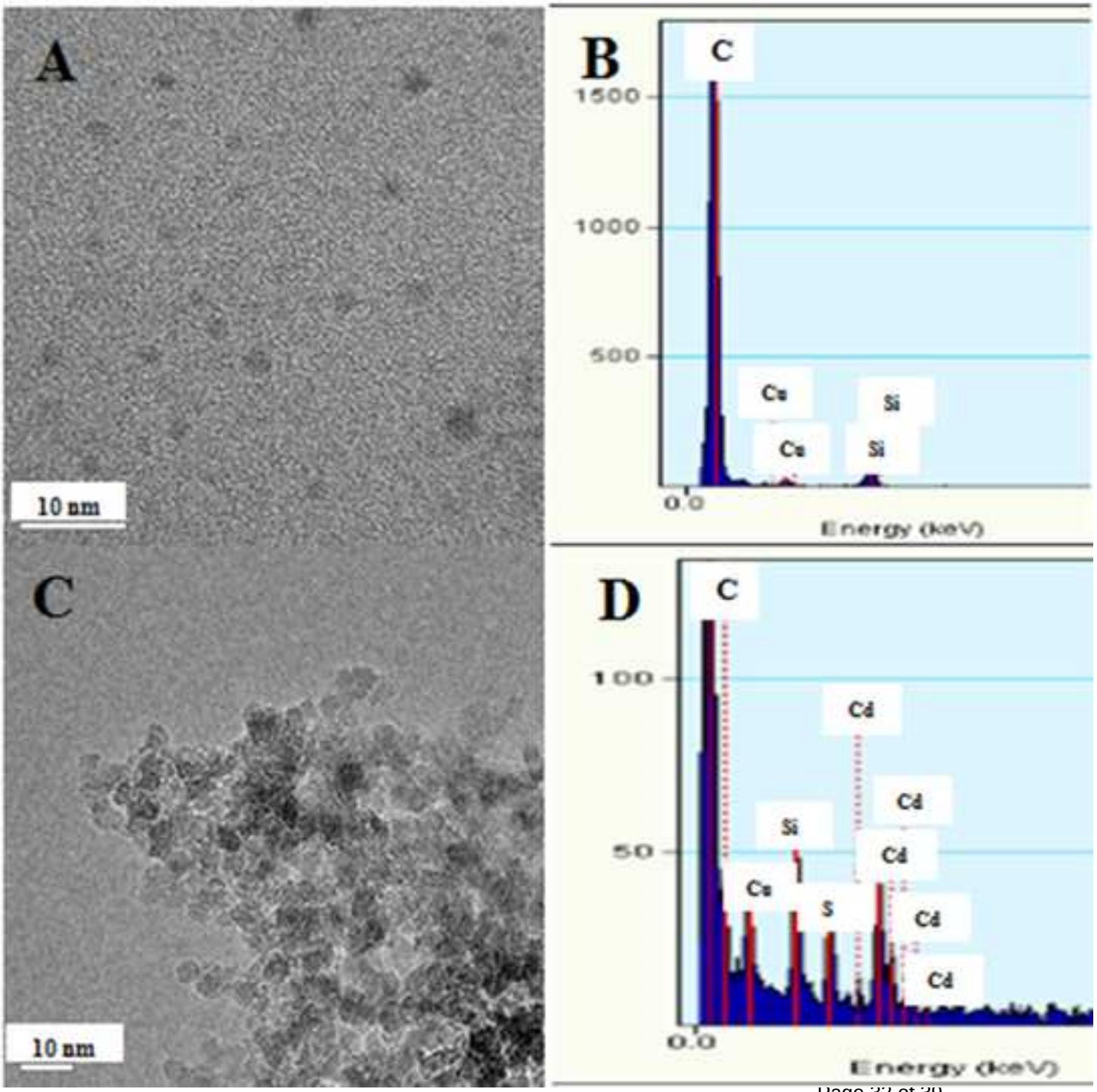

Figure 4

Click here to download high resolution image

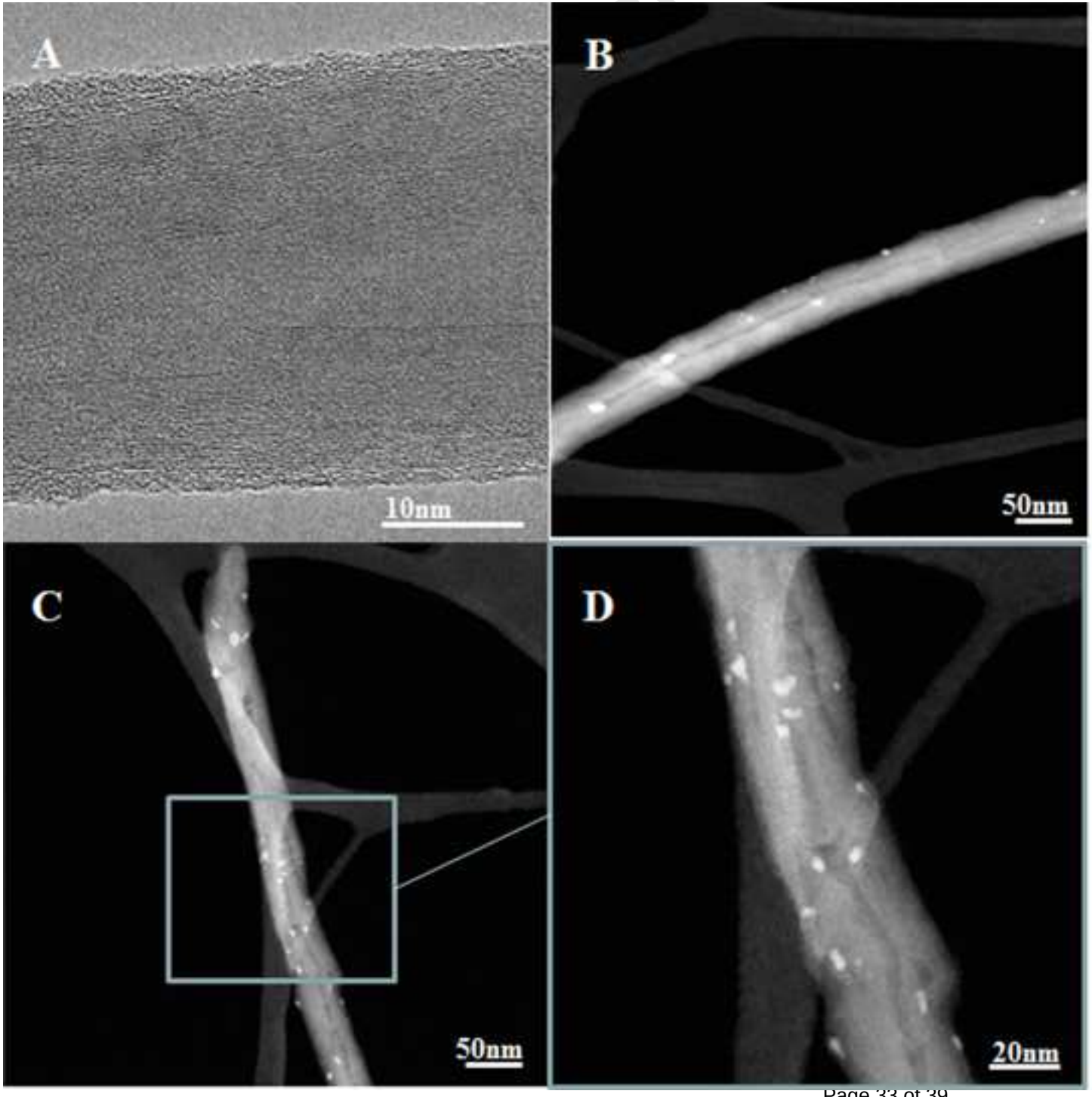

Figure 5

Click here to download high resolution image

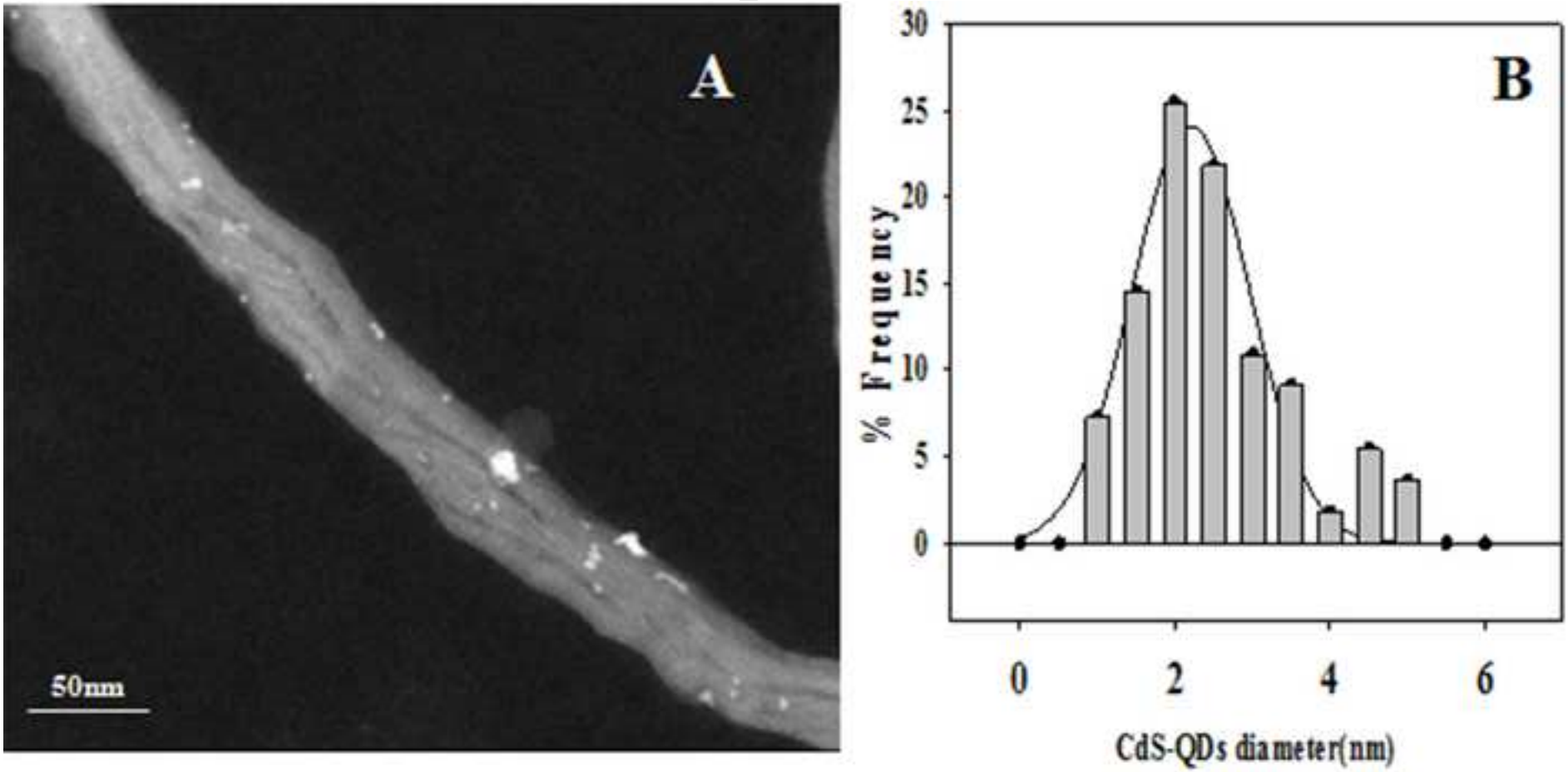

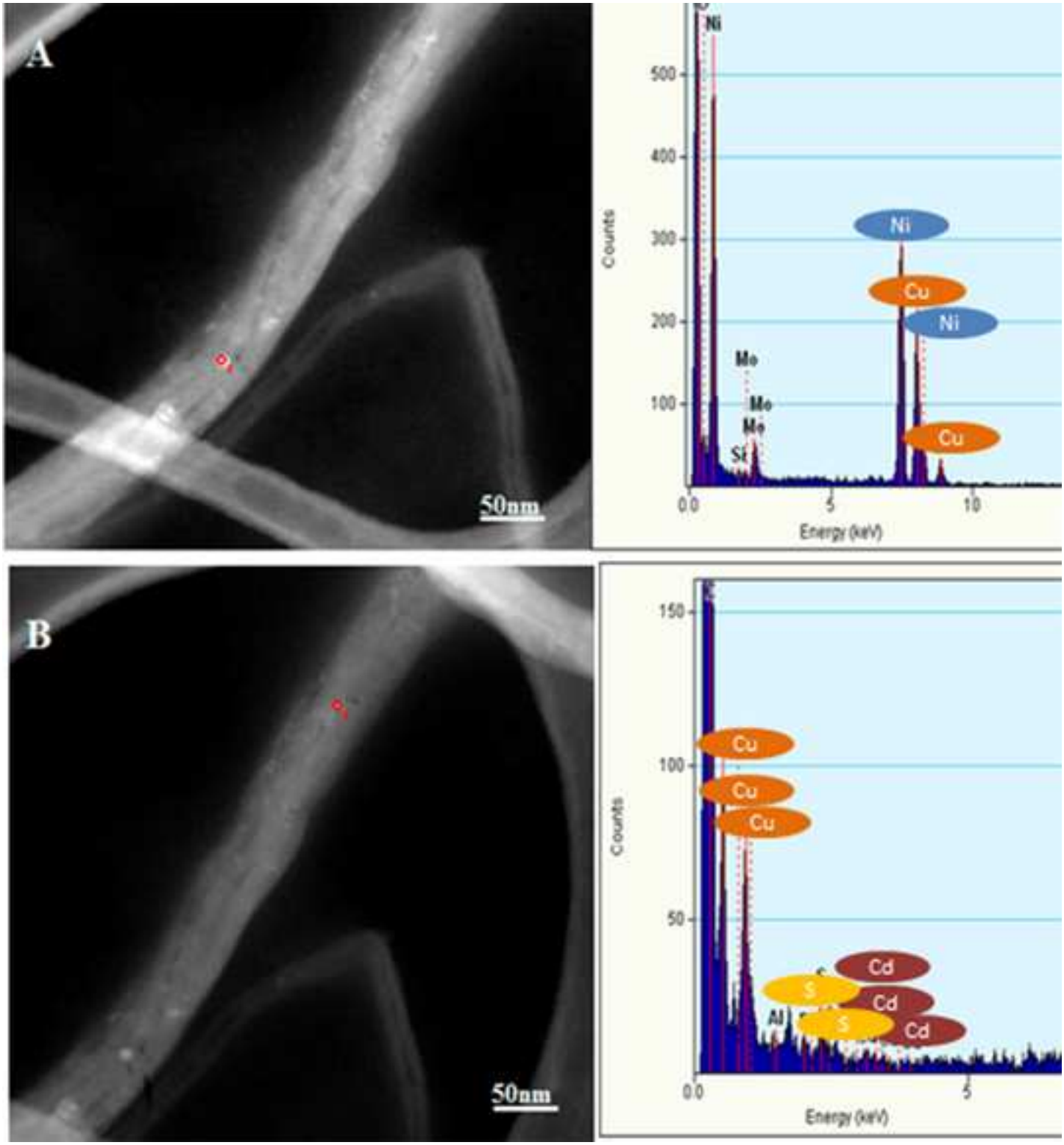

Figure 7

Click here to download high resolution image

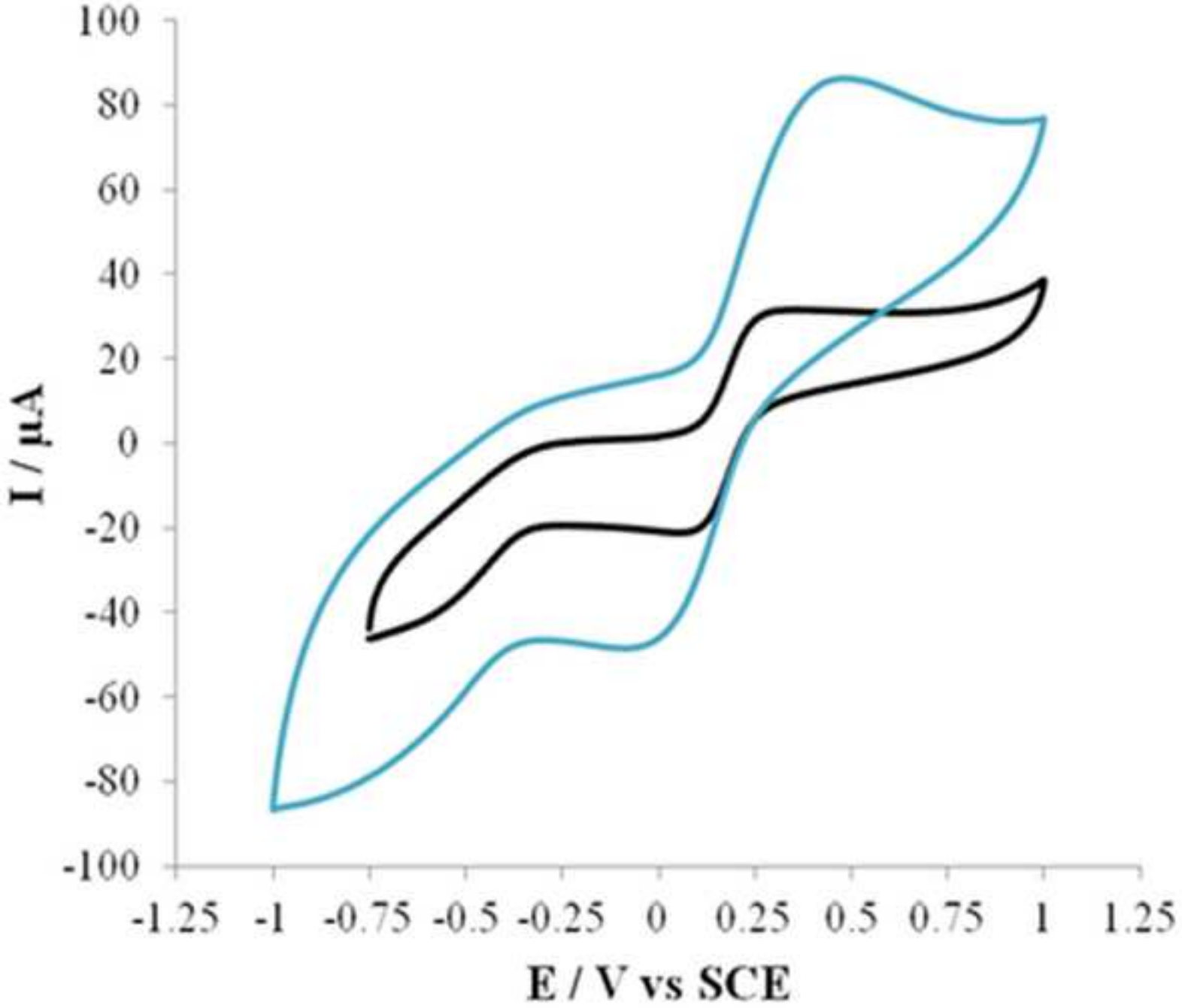

Figure 8

Click here to download high resolution image

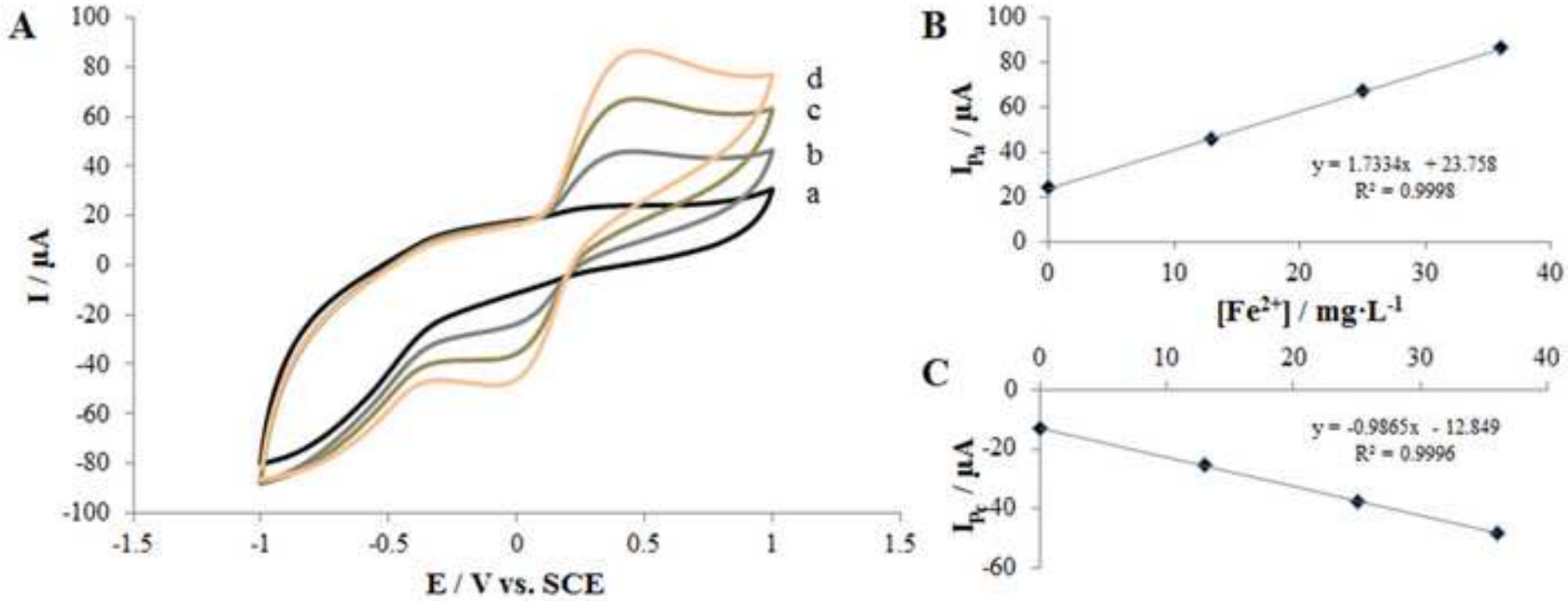

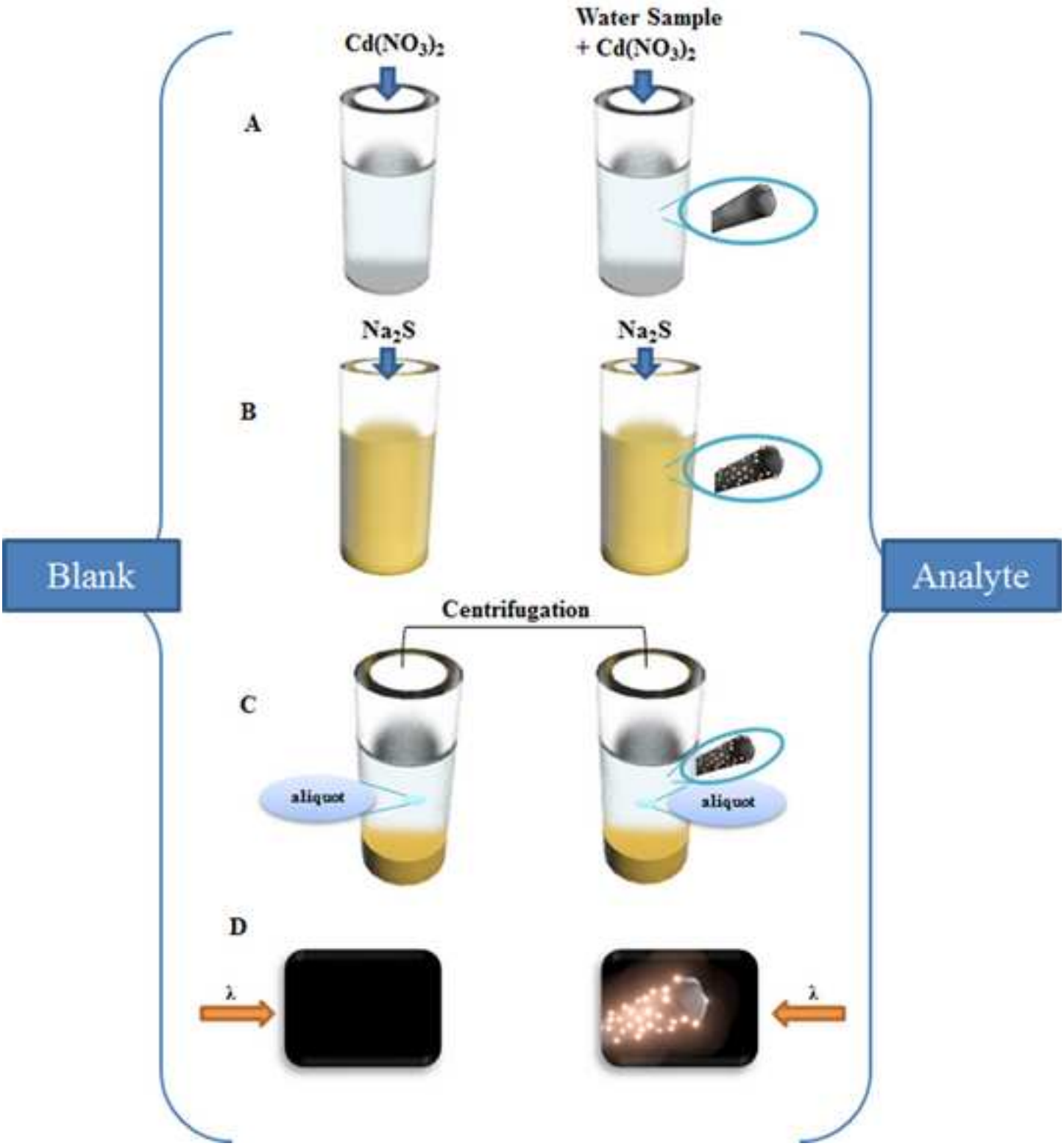
Water Sample
+ Cd(NO3)2
Cd(NO3)2
A
Na2S
Na2S
B
Blank
Analyte
Centrifugation
C
aliquot
aliquot
D
λ
λ

Figure 10

Click here to download high resolution image